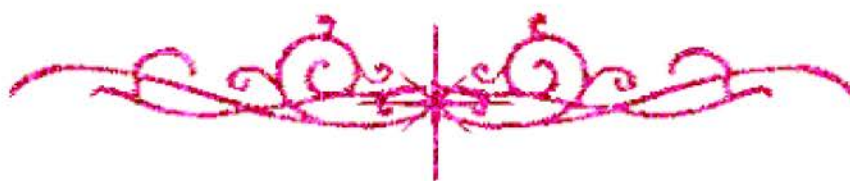


سامية محمد مصطفى



شبكة المعلومات الجامعية

بسم الله الرحمن الرحيم



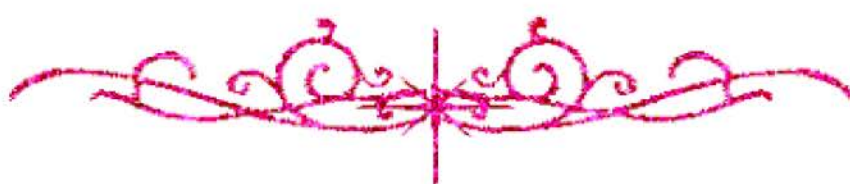
سامية محمد مصطفى



شبكة المعلومات الجامعية



شبكة المعلومات الجامعية التوثيق الالكتروني والميكرو فيلم



سامية محمد مصطفى



شبكة المعلومات الجامعية

جامعة عين شمس

التوثيق الإلكتروني والميكروفيلم

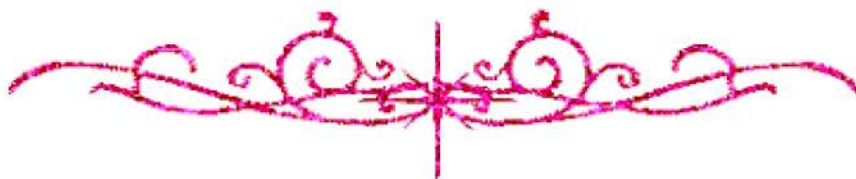
قسم

نقسم بالله العظيم أن المادة التي تم توثيقها وتسجيلها
علي هذه الأقراص المدمجة قد أعدت دون أية تغيرات



يجب أن

تحفظ هذه الأقراص المدمجة بعيدا عن الغبار



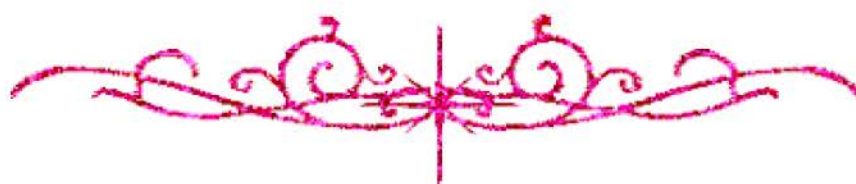
سامية محمد مصطفى



شبكة المعلومات الجامعية



بعض الوثائق الأصلية تالفة



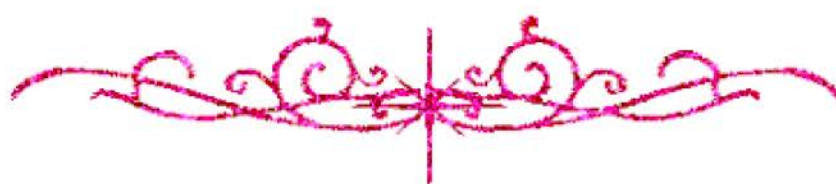
سامية محمد مصطفى

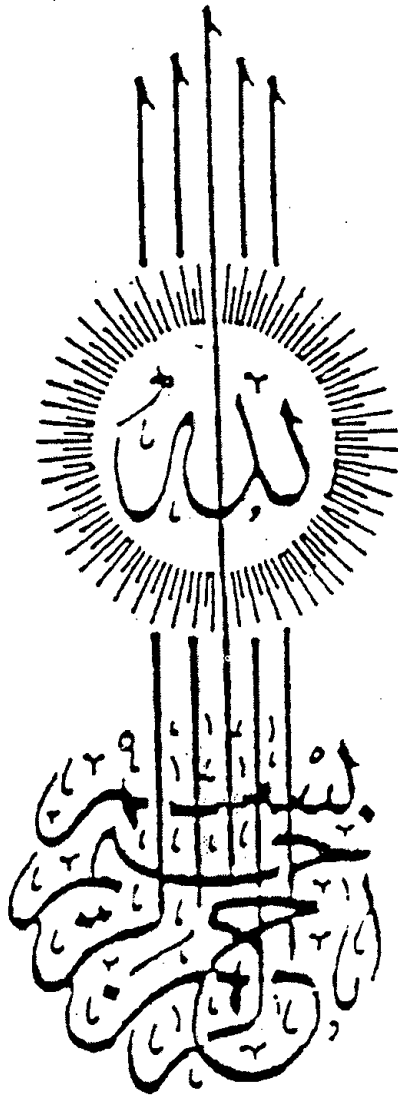


شبكة المعلومات الجامعية



بالرسالة صفحات لم ترد بالأصل





وَعَلَّمَكَ مَا لَمْ تَكُنْ تَعْلَمُ وَكَانَ فَضْلُ اللَّهِ عَلَيْكَ عَظِيمًا

صدق الله العظيم

B

١٣٩٧٠

***NEW APPROACHES TO INTERPRET
GRAVITY DATA***

A Thesis Submitted

To

Geophysics Department,

Faculty of Science, Cairo University

For the Degree of Doctor of Philosophy (Ph.D.)

in Geophysics (Potential Field Methods)

By

EID RAGAB ABD ELFATAAH ABO-EZZ

(B. Sc. in Geophysics, 1994)

(M. Sc. in Geophysics, 1999)

Giza, Egypt

2001

APPROVAL SHEET

TITLE OF THE Ph.D. THESIS

NEW APPROACHES TO INTREPRET GRAVITY DATA

Name of Candidate: *Eid Ragab Abd Elfataah Abo-Ezz*

Submitted to the Faculty of Science-Cairo University

Supervision Committee:

Prof. Dr. El-Sayed Mohamed Abdelrahman

*Professor of potential methods, Geophysics Department,
Faculty of Science, Cairo University*



Dr. Hesham Mohamed El-Araby

*Assistant Prof., Dept. of Geophysics,
Faculty of Science, Cairo University*




Dr. Tarek Mohamed El-Araby

*Lecturer, Dept. of Geophysics,
Faculty of Science, Cairo University*



Approved


Prof. Dr. El-Sayed M. Abdelrahman
Head of Geophysics Department
Faulty of Science, Cairo University

This thesis is dedicated to my professor E. M. Abdelrahman, Head and Chairman of Geophysics Department, Faculty of Science, Cairo University, for his continuous support during the progress of this thesis, his patience, his moral guidance and his superb way of supervision and without complaint.

ACKNOWLEDGMENTS

My great debt and sincere gratitude is due to almighty Allah who, in his infinite mercy and wisdom, made the completion of this thesis possible.

I am indebted to Prof. Dr. El-Sayed M. Abdelrahman, Head of Geophysics Department, and Professor of potential field methods, Geophysics Department, Faculty of Science, Cairo University, for his patience, his moral guidance, his superb way of supervision, continuous encouragement and technical review of the manuscript. I am also indebted to Dr. Hesham M. El-Araby, Assistant Professor of potential field methods, Geophysics Department, Faculty of Science, Cairo University, for his supervision and helpful advice during this thesis. I am also indebted to Dr. Tarek M. El-Araby, lecturer of potential field methods, Geophysics Department, Faculty of Science, Cairo University, for his supervision and helpful advice during this work.

It is my most pleasant duty to express my sincere gratitude to my family whose contribution cannot be put in words but can only be felt deeply in the heart.

TABLE OF CONTENTS

	page
ABSTRACT	1
GENERAL INTRODUCTION	4
<i>CHAPTER I</i>	
A GENERAL REVIEW OF REGIONAL-RESIDUAL SEPARATION, DEPTH, AND SHAPE ESTIMATION TECHNIQUES FROM GRAVITY DATA	6
INTRODUCTION	6
REVIEW OF THE PREVIOUS REGIONAL-RESIDUAL SEPARATION TECHNIQUES	6
1- Smoothing Techniques	9
2- Grid Method or Analytical Techniques	10
3- Least-Squares Methods:	12
REVIEW OF THE PREVIOUS DEPTH AND SHAPE ESTIMATION TECHNIQUES FROM GRAVITY DATA	13
<i>CHAPTER II</i>	
A NON-ITERATIVE APPROACH TO DEPTH DETERMINATION FROM RESIDUAL GRAVITY ANOMALY	18
INTRODUCTION	18
THE METHOD	19
DISCUSSION OF THE RESULTS	21
ANALYSIS OF THE METHOD	21

	Page
SYNTHETIC EXAMPLES	80
OPTIMUM-ORDER REGIONAL DETERMINATION	83
THEORETICAL EXAMPLES	84
APPLICATION TO FIELD EXAMPLE	96
<i>CHAPTER VI</i>	
SUMMMARY AND CONCLUSIONS	103
REFERENCES	105
APPENDCIES	113
APPENDIX I	113
APPENDIX II	116
APPENDIX III	119
APPENDIX IV	121
ARABIC SUMMARY	133

LIST OF FIGURES

	Page
Figure 1 The Karrbo gravity anomaly profile, Vastmanland, Sweden (Hedstrom, 1940 and Shaw and Agarwal, 1990).	27
Figure 2 Flow chart illustrating a generalized scheme for automated depth, shape, and amplitude coefficient estimation.	33
Figure 3 Error response in model parameters estimates. Abscissa: model depth. Ordinate: percent error in model parameters.	36
Figure 4 Gravity profiles and dome cross-section on line AA' of the Bouguer gravity map, Humble salt dome, Harris County, Texas, USA (Nettleton, 1976).	38
Figure 5 Composite gravity anomaly (Δg_1) of a buried vertical cylinder and first-order regional as obtained from equation (24).	47
Figure 6 Composite gravity anomaly (Δg_2) of a buried horizontal cylinder and second-order regional as obtained from equation (25).	48
Figure 7 Composite gravity anomaly (Δg_3) of a buried sphere and third-order regional as obtained from equation (26).	49
Figure 8 Second moving average residual gravity anomalies for $s=2,3$, and 4 km as obtained from gravity anomaly (Δg_1).	50
Figure 9 Second moving average residual gravity anomalies for $s=2,3$, and 4 km as obtained from gravity anomaly (Δg_2).	51
Figure 10 Second moving average residual gravity anomalies for $s=2,3$, and 4 km as obtained from gravity anomaly (Δg_3).	52
Figure 11 Family of window curves of Z as a function of q for $s=2,3$, and 4 km as obtained from gravity anomaly (Δg_1) using the present approach. Estimates of q and Z are, respectively, 0.5, and 2 km.	56

- Figure 12 Family of window curves of Z as a function of q for $s=2,3$, and 4 km as obtained from gravity anomaly (Δg_2) using the present approach. Estimates of q and Z are, respectively, 1.0 , and 4 km. 57
- Figure 13 Family of window curves of Z as a function of q for $s=2,3$, and 4 km as obtained from gravity anomaly (Δg_3) using the present approach. Estimates of q and Z are, respectively, 1.5 , and 6 km. 58
- Figure 14 Second moving average residual gravity anomalies for $s=2,3$, and 4 km as obtained from gravity anomaly (Δg_1) after adding 10% random errors to the data. 62
- Figure 15 Second moving average residual gravity anomalies for $s=2,3$, and 4 km as obtained from gravity anomaly (Δg_2) after adding 10% random errors to the data. 63
- Figure 16 Second moving average residual gravity anomalies for $s=2,3$, and 4 km as obtained from gravity anomaly (Δg_3) after adding 10% random errors to the data. 64
- Figure 17 Family of window curves of Z as a function of q for $s=2,3$, and 4 km as obtained from gravity anomaly (Δg_1) after adding 10% random errors to the data using the present approach. Estimates of q and Z are, respectively, 0.51 and 1.98 km. 66
- Figure 18 Family of window curves of Z as a function of q for $s=2,3$, and 4 km as obtained from gravity anomaly (Δg_2) after adding 10% random errors to the data using the present approach. Estimates of q and Z are, respectively, 1.1 and 4.4 km. 67
- Figure 19 Family of window curves of Z as a function of q for $s=2,3$, and 4 km as obtained from gravity anomaly (Δg_3) after adding 10% random errors to the data using the present approach. Estimates of q and Z are, respectively, 1.45 and 5.6 km. 68

	Page
Figure 20 Bougure gravity map, Humble salt dome, Harris County, Texas (Nettleton, 1962). Computations are made along profile AA.	69
Figure 21 Observed gravity profile on line AA of the Humble dome, near Houston, TX, U.S.A.	70
Figure 22 Second moving average residual gravity anomalies on line AA of the Humble dome, for $s=1.5, 1.75, 2$, and 2.25 km.	71
Figure 23 Family of window curves of Z as a function of q for $s=1.5, 1.75, 2$, and 2.25 km as obtained from the Humble gravity anomaly profile using the present approach. Estimates of q and Z are, respectively, 1.5 and 4.95 km.	72
Figure 24 Error response in depth parameter estimates. Abscissa: model depth. Ordinate: percent error in depth parameter.	81
Figure 25 Error response in amplitude coefficient parameter estimates. Abscissa: model depth. Ordinate: percent error in amplitude coefficient parameter.	82
Figure 26 Composite gravity anomaly (Δg_1) of a buried thin fault and a zero-order regional.	85
Figure 27 Composite gravity anomaly (Δg_2) of a buried thin fault and a first-order regional.	86
Figure 28 Composite gravity anomaly (Δg_3) of a buried thin fault and a second-order regional.	87
Figure 29 Gazelle fault gravity anomaly, south Aswan, Egypt.	98
Figure 30 Data analysis of Figure 29 using first-derivative method.	99
Figure 31 Data analysis of Figure 29 using second-derivative method.	100
Figure 32 Data analysis of Figure 29 using third-derivative method.	101
Figure 33 Data analysis of Figure 29 using fourth-derivative method	102